Journal of Applied Polymer Science

Improved Hemocompatibility of Silk Fibroin Fabric Using Layer-by-Layer Polyelectrolyte Deposition and Heparin Immobilization

M. Fazley Elahi,[1] Guoping Guan,[1] Lu Wang,[1] Martin W. King[1,2]

[1]Key Laboratory of Textile Science and Technology, Ministry of Education, College of Textiles, Donghua University, Songjiang District, Shanghai 201620, China

[2]College of Textiles, North Carolina State University, Raleigh, North Carolina 27695-8301

Correspondence to: L. Wang (E-mail: wanglu@dhu.edu.cn)

ABSTRACT: Silk fibroin has long been used as implantable surgical sutures and it has acceptable mechanical properties and patency rates in animal models and in clinical end-uses. However, fibroin has been shown to be hemolytic and can cause damage to red blood cells. So to be used as an implantable vascular prosthesis its hemocompatibility needs to be improved. This study has taken two sequential steps to address this problem. First, to create a positively charged layer on the fibroin fibers' surface, a 1.5 and 2.5 bilayers polyelectrolyte surface deposition layer-by-layer technique was used with the positive counterion poly(allylamine hydrochloride) and the negative counterion poly(acrylic acid). Second, negatively charged low molecular weight heparin was then immobilized on these positively charged self-assembled surfaces. The presence of the heparin was confirmed with Alcian Blue staining and a toluidine blue assay, and the increased roughness and hydrophilicity of the modified surfaces were characterized by scanning electron microscopy, contact angle measurements, and atomic force microscopy. In addition, a negligible hemolytic effect, reduced protein adsorption, and a higher concentration of free hemoglobin measured by a kinetic clotting time test were found to be enhanced with the use of 2.5 bilayers compared to the 1.5 bilayers self-assembly technique. Given the success of these preliminary results, it is anticipated that this novel approach of surface modification and heparin immobilization will demonstrate long-term patency during future animal trials of small caliber silk fibroin vascular grafts. © 2014 Wiley Periodicals, Inc. J. Appl. Polym. Sci. **2014**, *131*, 40772.

KEYWORDS: silk fibroin; polyelectrolye; layer-by-layer deposition; hemocompatibility; self-assembly

Received 10 January 2014; accepted 27 March 2014

DOI: 10.1002/app.40772

INTRODUCTION

Hemocompatibility is essential for biomedical devices used in direct contact with blood, such as, vascular grafts, artificial heart valves, and ventricular assist devices. However, major long-term complications for these devices, such as thrombosis, stenosis, embolization, and occlusion, still remain.[1] Current commercial synthetic grafts, fabricated from expanded polytetrafluoroethylene (ePTFE, Goretex®) and polyethylene terephthalate (PET, formerly Dacron®), are successful for the repair and replacement of the major caliber arteries, but fail for smaller diameters (<6 mm ID), such as coronary and femoral artery bypass procedures, due to thrombosis and/or compliance mismatch.[2–4] A number of different surface chemical and physical modification techniques have been developed and applied to synthetic grafts to engineer the material's surface properties to achieve the desired biocompatibility, biostability, and biofunctionality.

Silk fibroin (SF) is a natural protein material spun into filaments by the cultivated silkworm, *Bombyx mori*. It has been used in its native and regenerated form for many different biomaterial applications, such as sutures, cell culture media,[5] antithrombogenic materials,[6,7] wound dressings,[8] drug delivery carriers,[9–13] and scaffolds for tissue engineering[14,15] of bone[16–19] and cartilage.[20–22] Recent reports from our group and others have demonstrated that woven SF tubular fabrics provide a promising biomaterial for use as a small diameter arterial prosthesis.[4,23,24] Such graft materials fabricated from fibroin fibers provide excellent patency when implanted in the rat abdominal aorta, with 1 year patency rates of 85% which is much higher than for ePTFE (30%).[25] Unfortunately, native SF has a tendency to be hemolytic when used as a blood contacting material, in part, because the natural silk fibers are spun together with a coating of sericin gum which is known to damage red blood cells which lose their function.[26] Hence, the issue of how to improve the hemocompatibility of small diameter SF vascular grafts continues to be an important problem to be solved.

There are a few studies that have investigated the modification of SF fabrics using bioactive materials to improve their

© 2014 Wiley Periodicals, Inc.

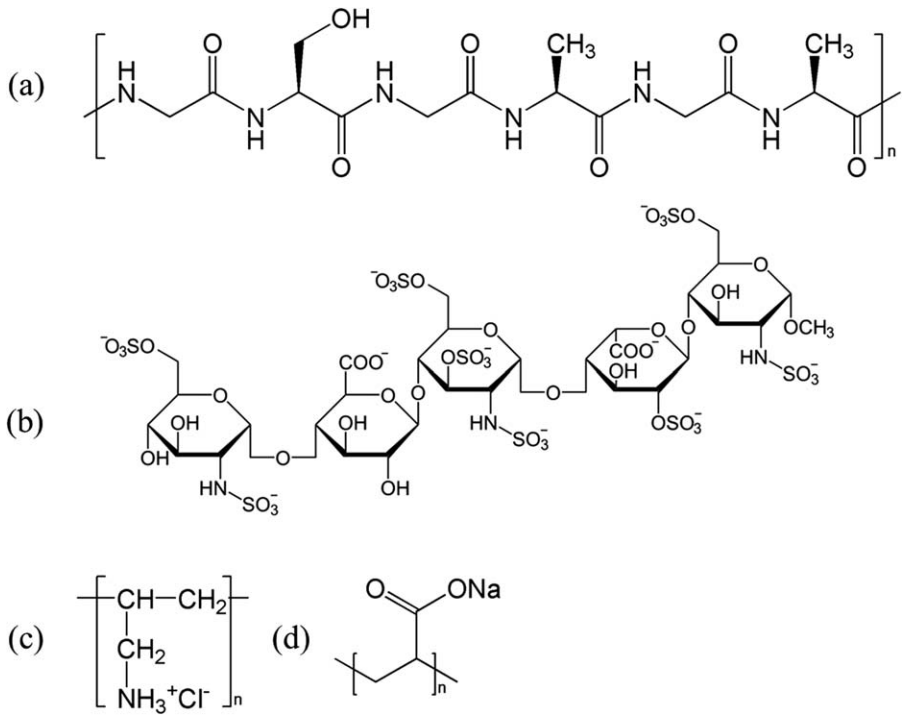

Figure 1. Chemical structures of the materials used: (a): SF, (b): low molecular weight heparin with two typical GAG repeats with multiple sulfate groups, (c): PAH, and (d): PAA.

hemocompatibility. In one of these studies, Wang et al.[27] modified the fibroin fabric with ferulic acid, and found that the activated partial thromboplastin time (aPTT), the prothrombin time, and thrombin time as well as the whole blood coagulant time of the modified fibroin fabrics were longer than that of pure SF. Furuzono et al.[7] grafted 2-methacryloyloxyethyl phosphorylcholine (MPC) onto fibroin fabric and observed that the number of platelets adhering to the polyMPC-grafted silk decreased by about one-tenth compared to the virgin fibroin fabric. Yagi et al.[28] coated a tubular raschel knitted silk vascular graft with an aqueous solution containing poly(ethylene glycol diglycidyl ether) and observed that *in vitro* there was no immediate thrombus formation.

To immobilize negatively charged low molecular weight heparin (LMWH) onto the surface there is first the need to create a suitable positively charged surface. It is therefore proposed in this study to modify the surface by applying a self-assembly technique using layer-by-layer polyelectrolyte deposition. LMWH was used as the anticoagulant agent because it is used effectively in the clinical for treating deep vein thrombosis and pulmonary embolism. It is an effective anticoagulant through binding to anti-thrombin (AT) which accelerates its inhibition of activated factor X (factor Xa).[29,30] Because of this LMWH cannot inhibit thrombin, but only inhibits clotting factor Xa. It has several advantages, such as its lower binding capacity to plasma proteins, platelets, and endothelium, longer half-life, lower risk of bleeding with a more predictable anticoagulant response compared with the use of unfractionated heparin.[31–33]

To immobilize negatively charged LMWH onto the SF surface, the self-assembly technique of using layer-by-layer polyelectrolyte deposition was selected to prepare a positively charged surface. In recent years, this technique has become one of the leading methods for the fabrication of nanoscale films with tailor-made properties.[34] The driving force for this layer-by-layer assembly approach is primarily electrostatic interaction, but the process can also involve charge-transfer interactions, van der Waals interactions, hydrogen bonding, and short-range hydrophobic interactions[35,36] between the layer to layer and the layer to substrate phases. One important feature of this method is the reaction at every step of a polyanion/polycation assembly, which results in recharging of the outermost layer during the fabrication process. The exact mechanisms that cause the formation of nanoscale films and composites with the base material is not yet clear, although a highly entangled and interpenetrating multilayer structure has been proposed.[37,38] The layer-by-layer assembly of oppositely charged polyelectrolytes on the substrate is facilitated by the formation of water-insoluble complexes of poly(allylamine hydrochloride) (PAH) and poly(acrylic acid) (PAA) via the ionic attractions between the carboxylate COO^- and ammonium NH_3^+ groups,[39,40] thereby improving the stability of the polyelectrolyte layers.

In this study, we have assembled 1.5 and 2.5 polyelectrolyte bilayers by ensuring that the positive counterion of PAH is on the outer layer of the modified fibroin followed by direct immobilization with the low molecular weight heparin (LMWH). Our objective was to prepare a flexible layer attached to the fibroin fabric with the ultimate goal of fabricating a flexible tubular vascular graft. To achieve this, we needed to use as few layers as possible. This is because it has been reported that multilayer layer-by-layer films are usually considered as rigid,

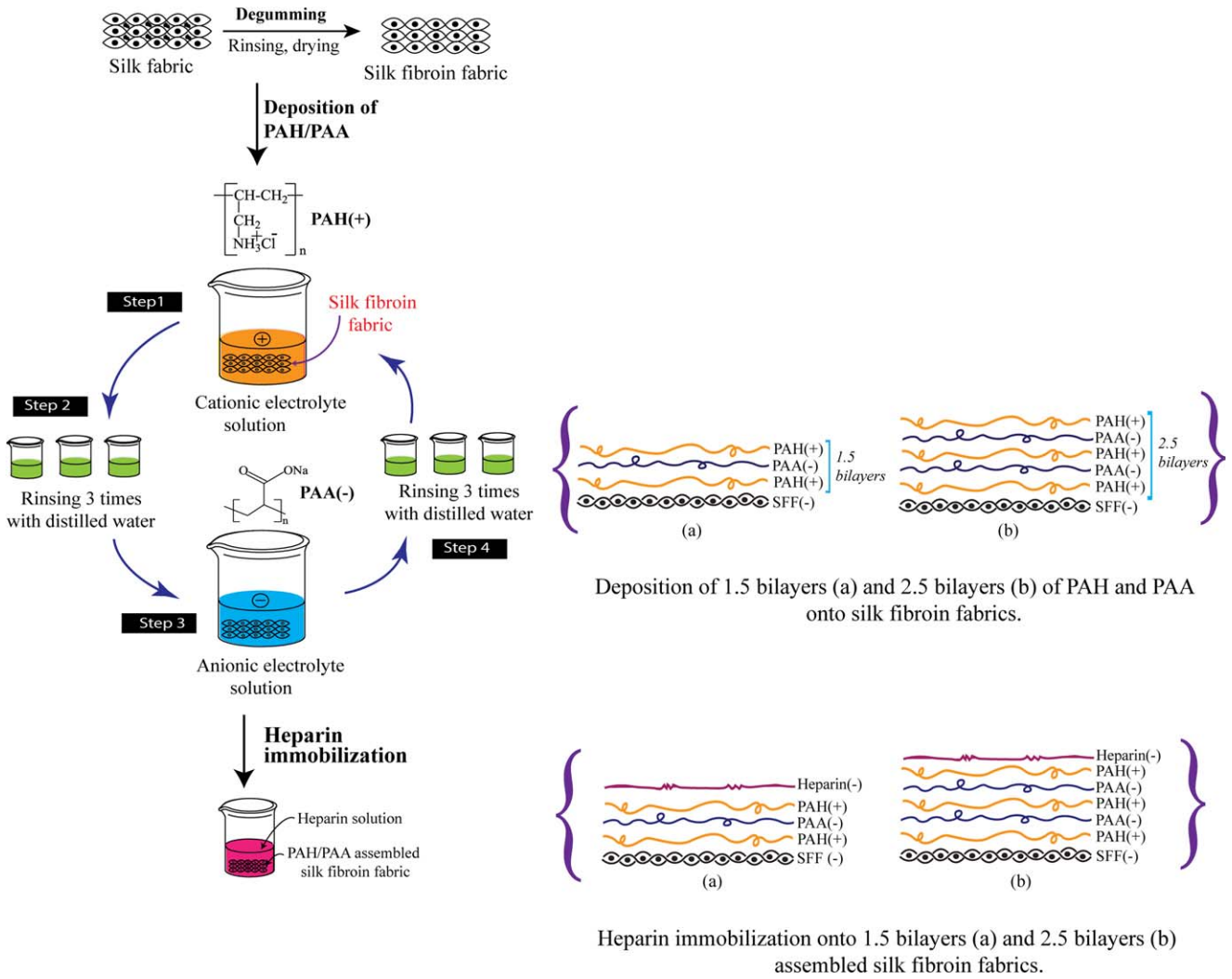

Figure 2. Diagram showing the deposition of PAH and PAA to create 1.5 and 2.5 polyelectrolyte bilayers on SF fabric surfaces followed by heparin immobilization. [Color figure can be viewed in the online issue, which is available at wileyonlinelibrary.com.]

nonflexible structures.[41] We predict that with the deposition of PAH and PAA layers and finally the immobilization of heparin onto the modified fibroin, we can obtain a stable heparinized surface, similar to that reported by Johansson et al., who deposited PAH on the outermost layer and was able to achieve superior adhesion.[42] This is the first study to immobilize heparin on a modified SF fabric using a layer-by-layer self-assembly technique to improve its hemocompatibility.

EXPERIMENTAL

Materials

Pure SF fabric derived from *B. mori* silkworms was supplied by Soho International Silk Company, Jiangsu Province, China. The fabric as received had been prepared by reeling and twisting the silk filaments surrounded by sericin gum, and weaving them into a 1/1 plain woven structure. Sodium carbonate (Na_2CO_3) was purchased as a powder from Biochemical Technology Company, Shanghai. Picric acid was supplied by Xilong Chemical Company, Shantou; and carmine by China National Medicines Company. Liquid ammonia was purchased from Kungshan Jingke Micro-electronics Material and hydrochloric acid (HCl) from Pinghu Chemical Reagent Factory, China. The calcium chloride ($CaCl_2$) used for the hemocompatibility test was purchased from Merck. Fetal bovine serum (FBS) and phosphate buffered saline (PBS) were purchased from Gibco (UK). Low molecular weight heparin (LMWH) (sodium salt, CAS 9041-08-1, $\geq$130 U/mg) and toluidine blue (CAS 92-31-9) were purchased from Sinopharm Chemical Reagent Company, Shanghai. The PAH (CAS 71550-12-4, average $M_w = 58{,}000$), and PAA (CAS 9003-01-4, average $M_w = 1800$), the Alcian blue 8GX, and bovine serum albumin (BSA) used for heparin staining were purchased from Sigma–Aldrich. The polyelectrolytes were used as received without further purification and were prepared as 1 gm/L solutions. Chemical structure of the basic materials used to perform the experiments is shown in Figure 1.

Preparation and Evaluation of Untreated Control SF Fabrics

The pure as received silk fabric was weighed and degummed by treating three times with 0.05% (w/w) Na_2CO_3 solution at 98°C to remove the associated sericin gum. Each alkaline procedure

Table I. Nomenclature Used for Untreated and Modified SF Fabric Samples

Samples ID	Preparation of the samples
SFF	Untreated SF fabric control
SFF-1	Deposition of 1.5 polyelectrolyte bilayers followed by heparin immobilized SF fabric
SFF-2	Deposition of 2.5 polyelectrolyte bilayers followed by heparin immobilized SF fabric

was 30 min long, followed by washing in distilled water and being allowed to dry at room temperature. The weight loss of silk fabric as a result of degumming was calculated as a percentage of the original weight. A qualitative evaluation of the effectiveness of the degumming process was performed using picric acid and carmine staining (PACS).[43] Briefly, a PACS solution was prepared by dissolving 1 g carmine in 10 mL 25% ammonia, adding 15 mL picric acid, before making up the solution to 100 mL with distilled water and adjusting the pH to 8.0–9.0 by the addition of hydrochloric acid. Samples of silk fabric before and after degumming were immersed in 1 mL PACS solution and heated in a boiling water bath for 5 min. At the end of this treatment, the fabrics were washed with distilled water and dried at room temperature. Digital images of the stained silk samples were obtained using optical microscopy (Nikon, Japan).

Deposition of Polyelectrolyte Bilayers on the Fibroin Fabric Surface

The concept for fabrication by the layer-by-layer process is shown in Figure 2. The 1.5 and 2.5 polyelectrolyte bilayers on the fibroin fabric surface were generated by sequential dipping of the substrate into aqueous solutions of PAH and PAA. The fibroin fabric was first immersed in an aqueous 1 mg/mL PAH solution and incubated at 37°C and 100 rpm for 30 min followed by rinsing three times, each time for 1 min in distilled water. The fabric was then immersed in an aqueous 1 mg/mL PAA solution for 30 min followed by the same rinsing steps in triplicate. The electrostatic adsorption and rinsing steps were repeated until the desired number of deposition bilayers (1.5 and 2.5) was obtained and the outermost layer was PAH. These modified fibroin fabrics containing the polyelectrolyte bilayers were dried at room temperature for 24 h prior to heparin immobilization.

Immobilization of Heparin onto Modified Fibroin Fabric Surfaces

A 1 mg/mL solution of LMWH was prepared by dissolving the powder in PBS solution. The modified fibroin fabrics were allowed to react with the heparin solution at 4°C for 24 h. After the immobilization reaction, the modified fibroin fabrics were washed with PBS and then rinsed with distilled water in an ultrasonic bath for 10 min. The nomenclature for the treated and untreated samples is listed in Table I.

Characterization Techniques

Fourier transformed infrared spectroscopy of the surface modified and untreated control fibroin fabrics was conducted on a Nicolet 6700 (Thermofisher) FTIR spectrophotometer fitted with an attenuated total reflectance (ATR) attachment for scanning in the range of 750–4000 cm^{-1}. The surface morphology and topography of the samples were observed by scanning electron microscopy (SEM) (Quanta-250, FEI) and atomic force microscopy (AFM) using a SPM Nanoscope IV instrument (Veeco Instruments). Water contact angle measurements were made with deionized water and an optical contact angle goniometer (Contact Angle System, Dataphysics Instruments GmbH, Germany). Five repeat measurements were made on different places on each sample. All the measurements were performed under ambient conditions.

Qualitative Characterization of Heparin

Alcian Blue staining was used to identify the presence of heparin retained on the substrate surfaces.[3] Briefly, the substrate was first treated with 10 mg/mL BSA in PBS at 37°C for 1 h and then rinsed with PBS three times. It was then stained with Alcian Blue 8GX (2%, w/v) diluted with 3% acetic acid solution at 37°C for 30 min and washed five times with distilled water. Finally the color intensity of the surfaces of the modified and untreated fibroin fabrics was observed by optical microscopy (Nikon, Japan).

Quantitative Characterization of Heparin

The amount of heparin immobilized on the polyelectrolyte deposited fibroin fabrics was determined quantitatively by the method reported by Park et al.[44] To establish a standard curve,

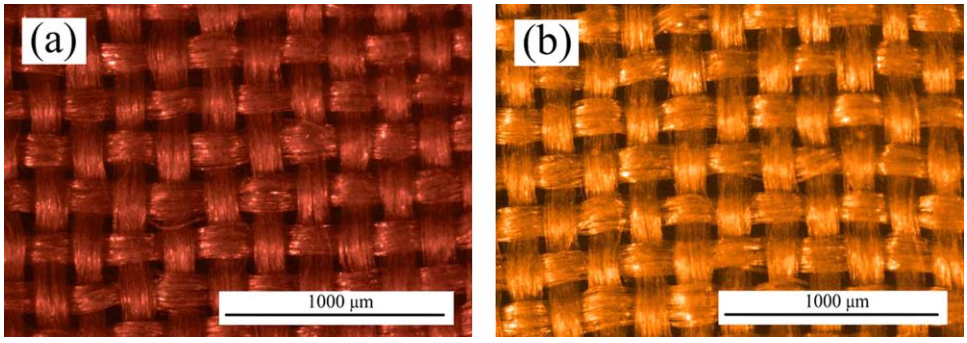

Figure 3. Picric acid and carmine staining: (a): the as received silk fabric is dark red which suggests that sericin is coating the silk fibers, (b): the alkali degummed silk fabric displayed a yellow color implying the removal of sericin. [Color figure can be viewed in the online issue, which is available at wileyonlinelibrary.com.]

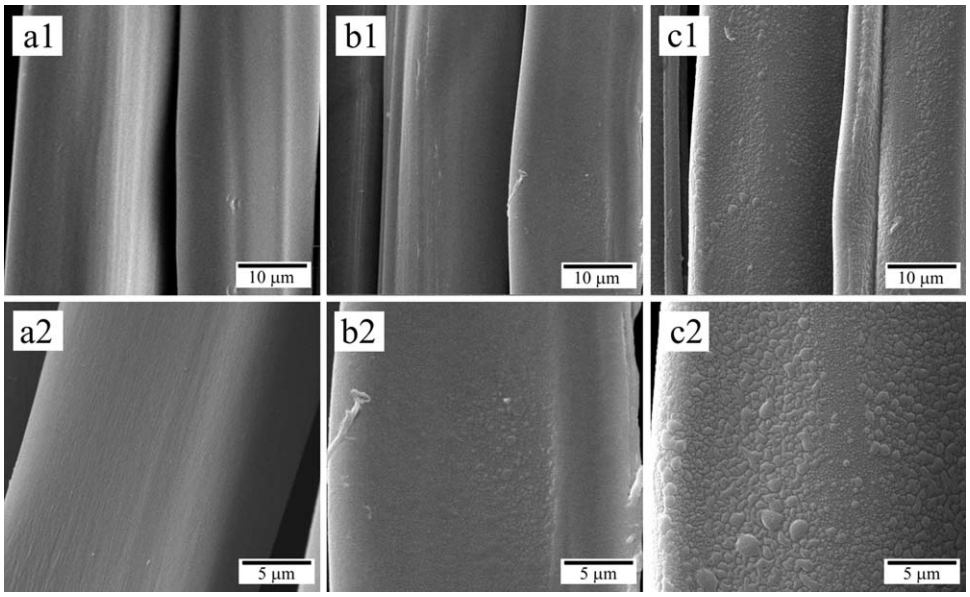

Figure 4. SEM micrographs of untreated and modified SF fabrics: (a1, a2): SFF, (b1, b2): SFF-1, and (c1, c2): SFF-2. Magnification: top row ×5000; bottom row ×10,000.

a range of concentrations (5–35 mg/mL) of heparin solution (2.0 mL) was prepared in separate 10 mL conical flasks. A volume of 3 mL of toluidine blue solution (25 mg toluidine blue dissolved in 500 mL 0.01*M* HCl containing 0.2% NaCl) was added to each flask, which was then shaken to ensure complete reaction. After 30 min, 3 mL *n*-hexane was added to the solution, mixed, and allowed to phase-separate. The heparin/toluidine blue complex that formed was extracted with the *n*-hexane and its concentration was determined using a UV–visible spectrophotometer (Perkin Elmer Lambda 25) at a wavelength of 631 nm. The calibration curve for relating the absorbance measurement to the concentration of heparin was then established. For measuring the amount of heparin immobilized on the surface of the fibroin fabrics, 2 mL of distilled water and 3 mL of toluidine blue solution were added to an empty 10 mL conical flask. Samples of the heparin immobilized fibroin fabric measuring 1 cm × 1 cm were then immersed in the solution and the reaction was allowed to continue for 30 min. After that, 3 mL of *n*-hexane was added to the flask, which was shaken to accelerate the extraction of the heparin/toluidine blue complex by the *n*-hexane. By measuring the absorbance of the aqueous solution at 631 nm, the amount of heparin on the surface of the fibroin fabric samples was quantified. This analysis was undertaken in triplicate and the average results are presented in the results section.

Stability Test of Immobilized Heparin

The heparin immobilized SF fabrics (SFF-1 and SFF-2) measuring 1 cm × 1 cm were then immersed in a beaker containing 50 mL PBS (pH 7.4) at room temperature for 24 h. Two fabric specimens were taken out at predetermined times (t =3, 6, 9, 12, 18, 19, and 24 h) and the amount of heparin remaining on these samples was determined using the toluidine blue method. The release of heparin can be calculated according to eq. (1).[45]

$$\text{Release of heparin (\%)} = \frac{D1-D2}{D1}\times 100, \quad (1)$$

where $D1$ and $D2$ are the surface densities of LMWH on the modified silk fabrics before and after extraction with PBS solution, respectively.

Protein Adsorption Assay

A protein adsorption assay was undertaken to determine if the fibroin fabric's affinity for blood plasma proteins was altered as a result of the surface modification. Less protein adsorption is believed to be advantageous for blood-contacting materials. Before exposing the untreated and surface modified fibroin samples and the glass cover slip controls to FBS, they were all sterilized by exposure to 75% aqueous ethanol for 1 h and soaked in PBS solution for an additional 2 h. The sterile samples were then placed in triplicate in a 24-well tissue culture plate and incubated with 1 mL FBS (10%) solution for 24 h at 37°C. The concentrations of FBS were measured before and after adsorption using a Lambda 25 UV–visible spectrophotometer (Perkin Elmer Lambda 25) at 280 nm with the aid of a standard FBS calibration curve that had been established previously.

Hemolytic Assay

Citrated human whole blood anti-coagulated with 3.8% sodium citrate solution, giving a whole blood to citrate solution ratio of 9 : 1 (v/v), was kindly provided by Shanghai First People's Hospital (Shanghai, China). To completely remove the serum, the blood was centrifuged and washed with PBS five times using a Biofuge Primo Model R centrifuge following standard procedures reported in the literature.[46,47] The separated red blood cells were first suspended by diluting 35 times in PBS solution. This meant that 1 mL of human red blood cells (HRBCs) was added with 34 mL PBS. Then 0.2 mL of the HRBCs suspension was transferred to a 5 mL Eppendorf tube, which was filled

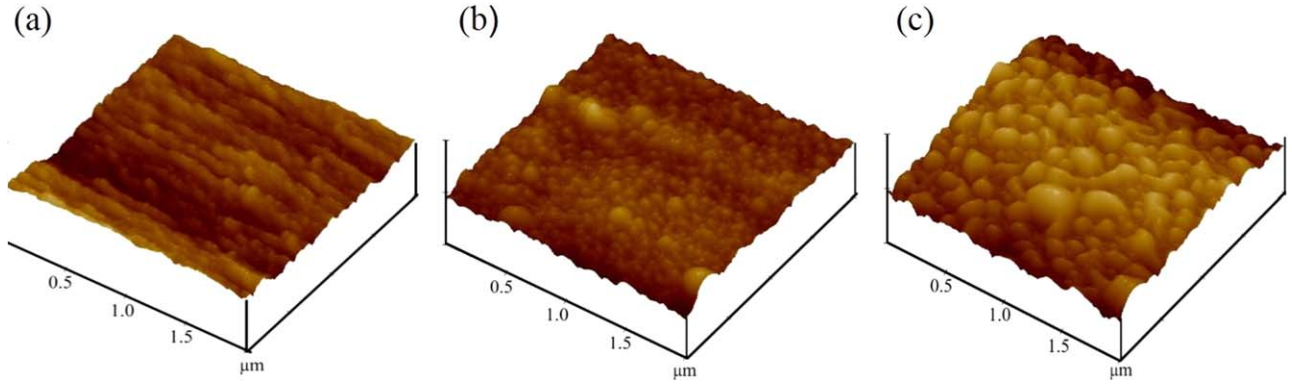

Figure 5. AFM images of untreated and surface modified SF fabrics: (a): SFF, (b): SFF-1, and (c): SFF-2. [Color figure can be viewed in the online issue, which is available at wileyonlinelibrary.com.]

with either 0.8 mL of deionized water as the positive control, or PBS buffer as the negative control.

Both the untreated and surface modified fibroin fabric samples were incubated in the suspension containing 0.2 mL diluted HRBC and 0.8 mL PBS buffer at 37°C for 2 h, followed by centrifugation (10,000 rpm; 3 min) in an Eppendorf 5415 Model R centrifuge. Then the optical density of the supernatant was determined by a Perkin Elmer Lambda 25 UV–visible spectrophotometer operating at 540 nm. The hemolysis percentage (HP) was calculated using eq. (2).[48,49]

$$\text{HP}\ (\%) = \frac{(D_t - D_{\text{nc}})}{(D_{\text{pc}} - D_{\text{nc}})} \times 100, \qquad (2)$$

where D_t is the absorbance of the test sample, and D_{pc} and D_{nc} are the absorbances of the positive and negative controls, respectively.

Rate of Coagulation Assay

The rate of coagulation of the untreated and modified fibroin fabrics was determined by a kinetic clotting time method that has been described previously.[50,51] To perform this assay, the untreated, surface modified, and heparin immobilized fibroin fabric samples were cut into small squares measuring 20 × 20 mm^2 and were put in triplicate into individual wells in a 12-well tissue culture plate. Glass cover slips were added to some of the wells as a positive control. Then anticoagulated whole human blood (20 μL) was dropped onto the surface of the fabric samples and the glass cover slip controls. To start the blood coagulation cascade, 10 μL of $CaCl_2$ solution (0.2 mol/L) was added to the blood in each well and incubated at 37°C for one of the predetermined periods of time, either 5, 10, 20, 40, or 60 min. Then 5 mL distilled water was carefully placed in each well and incubated at 37°C for 5 min. The concentration of free hemoglobin in the aqueous blood solution was measured by determining the optical density at 540 nm using a Lambda 25 UV–visible spectrophotometer (Perkin Elmer). It has been shown that red blood cells trapped inside a fibrin clot will not release their hemoglobin as rapidly as those mobile cells that are not part of the thrombus.[49] As a result, the rate of thrombus formation can be monitored indirectly by measuring the concentration of free hemoglobin in the diluted blood sample following incubation and clotting for specific periods of time.

In preparation for SEM, the samples were fixed in 2% buffered glutaraldehyde solution in a refrigerator at 4°C for 30 min, dehydrated by a series of solutions with increasing ethanol concentration (i.e., 55%, 70%, 80%, 90%, 95%, and 100%) and then dried in a desiccator. Before viewing in the SEM, the samples are coated with gold-palladium during a 60 s sputter-coating procedure.

Statistical Analysis

The data are reported as means and standard deviations, and the error bars in the figures correspond to one standard deviation. All the statistical analyses were performed using a one way analysis of Variance (ANOVA) statistic. A P value of <0.05 was selected as the confidence interval where differences were first found to be significant. The data in the tables are indicated with (*) for $P < 0.05$, (**) for $P < 0.01$, and (***) for $P < 0.001$.

RESULTS AND DISCUSSIONS

Degumming Efficiency

To confirm the effectiveness of the alkali treatment for silk fabric degumming, picric acid and carmine staining (PACS) were used. Fibroin selectively adsorbs picric acid molecules in alkaline solution, generating a yellow color. However, both carmine and picric acid can adhere to sericin simultaneously because of its stronger adsorptive properties. When sericin is present on silk fibers, the silk will be stained red because the red color is more dominant than the yellow color. Therefore, if silk turns yellow after being dyed, this suggests that all sericin has been completely removed.[43] Figure 3 shows the as received silk fabric stained dark red, indicating the presence of sericin surrounding the silk fibers [Figure 3(a)]. Conversely, the silk sample that had been degummed by the alkali treatment [Figure 3(b)] displayed a yellow color implying that the sericin had been removed. In

Table II. Surface Roughness of Untreated and Modified SF Fabric Samples

Samples ID	Maximum height of roughness (nm)
SFF	78.39
SFF-1	108.42
SFF-2	116.35

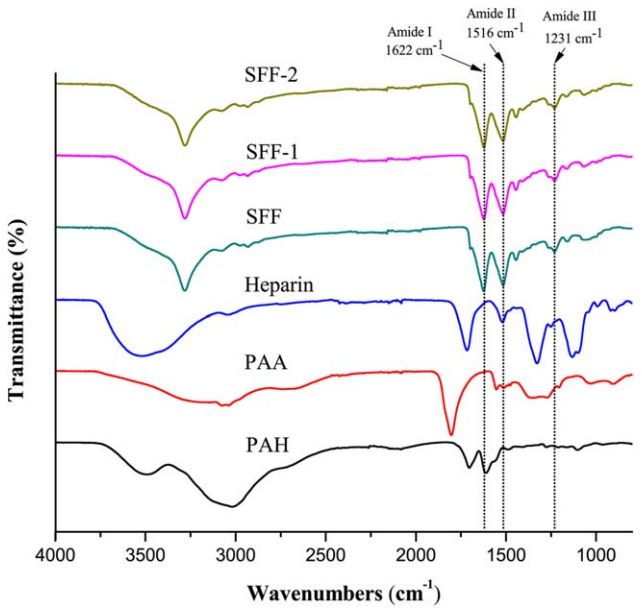

Figure 6. FTIR spectra of SFF-2, SFF-1, SFF, Heparin, PAA, and PAH. [Color figure can be viewed in the online issue, which is available at wileyonlinelibrary.com.]

addition, gravimetric measurements, which represent a quantitative assessment of the degumming process, gave a value for the weight loss of the degummed silk fabric of 25.5%.

Surface Morphology

The morphology and topography of the untreated and modified fibroin fabrics were observed by SEM and AFM. SEM micrographs of untreated and modified SF fabrics are shown in Figure 4. The surfaces of the modified fibroin materials changed from being smooth [Figure 4(a1,a2)] to being irregular and rough [Figure 4(b1,b2,c1,c2)]. This suggests that the polyelectrolyte multilayers and heparin were not uniformly deposited and distributed on the fabric surfaces. In fact, because the surface of the SFF-2 sample, with 2.5 bilayers of polyelectrolyte, was found to be rougher than the SFF-1 sample, the roughness of the fabrics appeared to increase with additional polyelectrolyte layers.

It was noted that on washing in an ultrasonic bath, only a small amount of heparin was released. In fact most of the heparin remained attached to the polyelectrolyte modified surface, which suggests that good bonding occurred between the LMWH and the layer-by-layer modified fibroin fabric with an increasingly rougher surface morphology.[52] This may be a case where the increasing number of both positive and negative electrolytes creates more polar radicals and functional groups on the surface, which in turn simply promotes stronger binding of the negatively charged heparin molecule. However, the increased thickness of the polyelectrolyte layers may also provide the heparin molecule with some additional or alternative conformations in which to form and attached to the modified fibroin surface at a lower energy state.

The typical AFM images taken of the untreated and treated fibroin fabrics are shown in Figure 5. The surface topography of the fibroin samples appeared to change qualitatively as a result of surface modification. Before modification, the top view of the fibroin surface appeared to be comparatively smooth. After modification, the fiber surfaces became more uneven with many convex protrusions separated by pits or valleys, suggesting that the polyelectrolyte deposition caused irregular condensation clusters on the fibers' surface. Table II shows the maximum height of the surface roughness of the untreated and surface modified fibroin fabrics according to AFM analysis.

FTIR-ATR

FTIR was used to assess any significant changes in the chemistry and fine structure of the fibroin biopolymer material as a result of the polyelectrolyte deposition process. Figure 6 shows the amide I band absorption at 1622 cm^{-1} (~80% CO stretching, ~10% CN stretching, ~10% NH bending vibration), the amide II absorption band at 1516 cm^{-1} (~60% NH bending vibration, 40% CN stretching), and the amide III band absorption at 1231 cm^{-1} (30% CN stretching, 30% NH bending vibration, 10% CO stretching, 10% O═C─N bending vibration). The above absorption bands are attributed to the β-sheet structure of the SF (Figure 1).[53] No infrared peaks were observed to shift between the untreated and the surface modified fibroin samples, confirming that there were no conformational changes in the chemical structure of the bulk fibroin. These results agree with the findings reported previously on the FTIR analysis of silk scaffolds and vascular grafts containing heparin.[11,54] The sampling depth of the FTIR technique is in the order of several

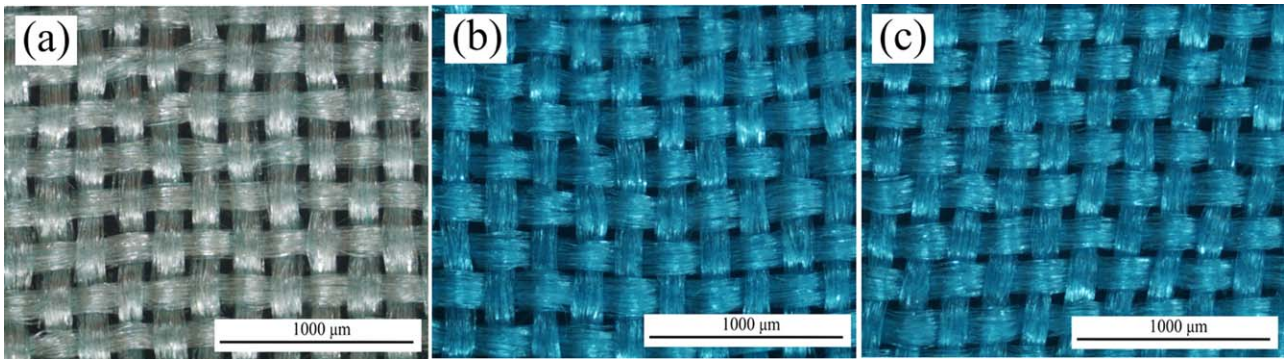

Figure 7. Optical microscopy images of Alcian blue stained untreated and surface modified SF fabrics. Magnification: ×40. (a): SFF, (b): SFF-1, and (c): SFF-2. [Color figure can be viewed in the online issue, which is available at wileyonlinelibrary.com.]

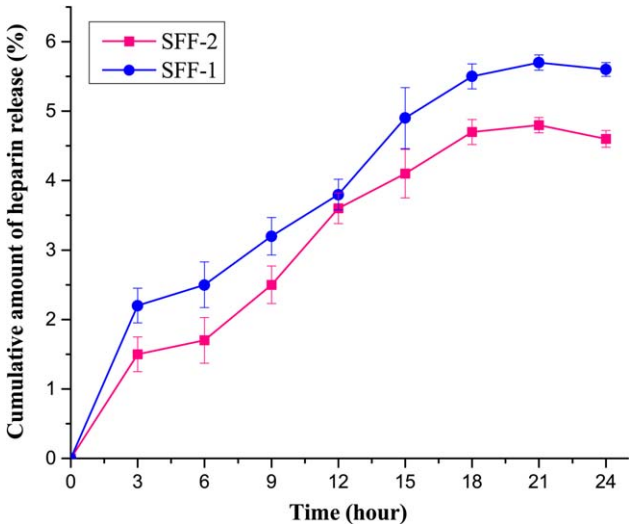

Figure 8. Heparin release (%) from surface modified SF fabrics. [Color figure can be viewed in the online issue, which is available at wileyonlinelibrary.com.]

microns depending of the wavelength of the incident beam. Positive identification of the nanometer thick polyelectrolyte deposition layers and the heparin layer was therefore not expected.

Qualitative and Quantitative Characterization of Heparin

Figure 7 shows the Alcian blue stained untreated and modified SF fabrics. Alcian Blue is a cationic dye, which can be used to selectively stain anionic glycosaminoglycans (GAGs) such as hyaluronan or heparin. After the immobilization of heparin and Alcian Blue staining, an evident difference in color was observed by light microscopy between the untreated [Figure 7(a)] and treated fibroin fabric surfaces [Figure 7(b,c)]. This result confirms the presence of an active GAG such as heparin and indicates that it is uniformly distributed over the surface of the modified fibroin fabrics. According to the toluidine blue quantitative assay, the average heparin content was found to be 15.34 $\mu g/cm^2$ and 13.38 $\mu g/cm^2$, respectively, for the SFF-1 and SFF-2 samples.

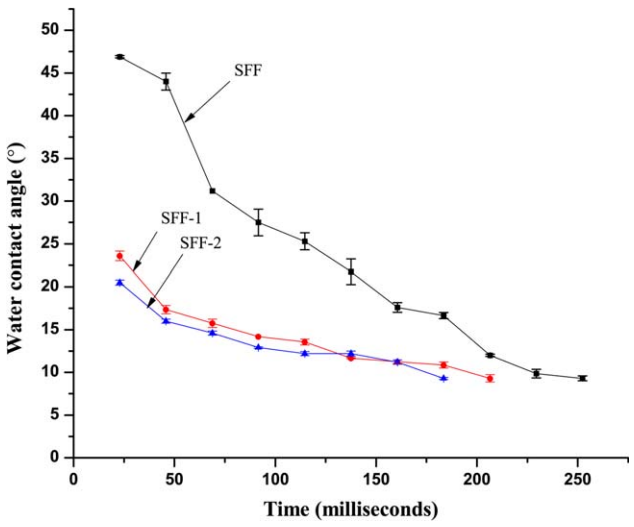

Figure 9. Average dynamic water contact angle of the untreated and surface modified SF fabrics measured during the initial 250 ms of the test. Data are shown as mean ($n = 5$), and the ± error bars = 1 standard deviation. [Color figure can be viewed in the online issue, which is available at wileyonlinelibrary.com.]

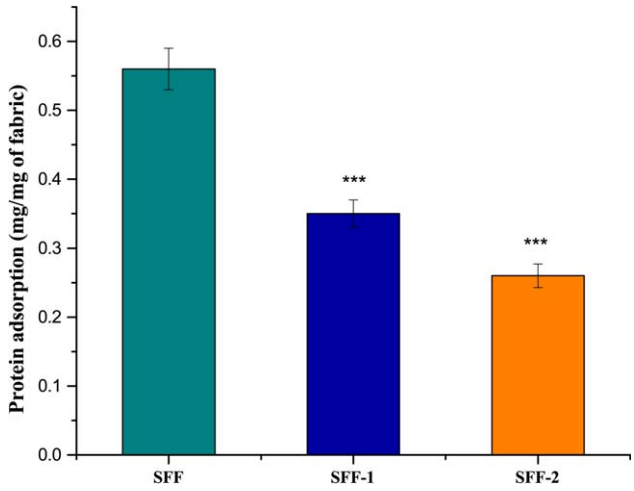

Figure 10. Average amount of plasma proteins adsorbed (mg protein per mg substrate) on the untreated and modified fibroin fabrics. Statistical differences between the untreated (SFF) control and the modified fibroin fabrics are indicated with (*) for $P < 0.05$, (**) for $P < 0.01$, and (***) for $P < 0.001$, respectively. Data for each sample are expressed as the mean ($n = 3$), and the ± error bars = 1 standard deviation. [Color figure can be viewed in the online issue, which is available at wileyonlinelibrary.com.]

Stability Test of Immobilized Heparin

The percent release of heparin from the two surface modified and heparin immobilized fibroin fabric samples is shown in Figure 8. The amount of heparin released gradually increased

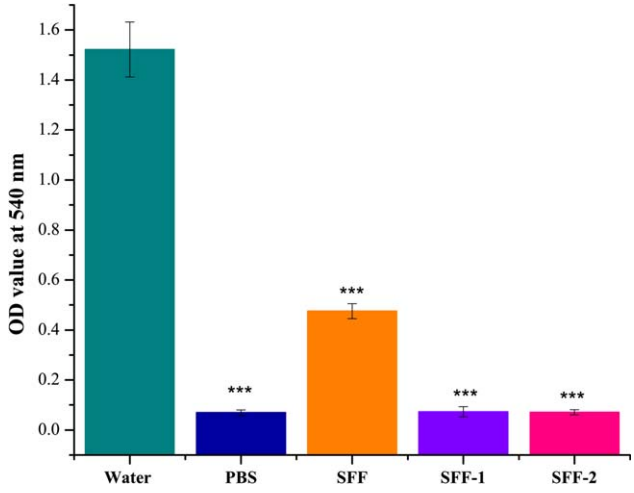

Figure 11. Mean hemolytic assay results showing HRBC exposure to the untreated (SFF) and modified fibroin fabric samples (SFF-1 and SFF-2) compared to the PBS solution negative control and the water positive control. Mean data for each sample ($n = 3$), and the ± error bars = 1 standard deviation. Statistical differences indicated (***) for $P < 0.001$. [Color figure can be viewed in the online issue, which is available at wileyonlinelibrary.com.]

Table III. HP of Untreated and Modified SF Fabric Samples

Samples	SFF	SFF-1	SFF-2
HP (%)	7.31 ± 1.27	0.24 ± 0.02	0.09 ± 0.01

with the duration of immersion time. After 18 h immersion, the maximum release of heparin was found to be around 4.5–5.5%. And after that the curve was stabilized with no further release of heparin. The small portion of heparin loss was probably due to non-immobilized physically adsorbed heparin on the fibroin fabric surfaces. It may also be assumed that the higher heparin % release observed in SFF-1 as the heparin was not attached strongly onto SFF-1 compared to SFF-2. It could be considered that the 2.5 bilayers deposited SF fabric have strong heparin binding capacity than the 1.5 bilayers deposited SF fabric. The fact that about 95% of the immobilized heparin could withstand 24 h of PBS solution extraction, points to effective bonding via polyelectrolyte assembly between the heparin and the modified fibroin fabric. This result is in agreement with the previously reported data.[45,55]

Water Contact Angle Results

The wettability of a biomaterial's surface contributes to its overall hemocompatibility as it influences the extent of protein adsorption, platelet adhesion, and activation, as well as its blood coagulation properties.[56] However, observations regarding the effects of surface wettability on protein adhesion have not always been consistent. In general, hydrophobic surfaces are considered to be more attractive for protein adsorption than hydrophilic surfaces because of the stronger hydrophobic interactions occurring at these surfaces in direct contrast to the repulsive solvating forces arising from strongly bound water on a hydrophilic surface.[56–58] The average dynamic contact angle measurements taken during the initial 250 ms acquisition times for all three types of fibroin fabric samples are presented in Figure 9. As one can see, as time increased, the contact angles showed a tendency to decrease for both the untreated and treated fabrics.

The maximum water contact angle of about 47° was found for the untreated fibroin fabric compared to the lower values of 23.6° and 20.6° for the modified SFF-1 and SFF-2 surfaces, respectively. It took about 250 ms for the untreated control sample to reach a contact angle of 9°, while both modified fabrics achieved a contact angle of 9° in a shorter time. For the SFF-1 sample, it took almost 205 ms to reach 9°, whereas for the SFF-2 fabric it needed only 183 ms. The addition of functional groups such as COO^- and NH_3^+ during the polyelectrolyte self-assembly process could be the major reason for the improved surface hydrophilicity of the modified fibroin fabrics. The hydrophilicity was further improved by the immobilization of heparin, which being a sulfated glycosaminoglycan, contained hydrophilic groups, such as sulfonic acid, carboxyl acid, and hydroxyls, within its structure (Figure 1). As the hydrophilicity of the heparin immobilized samples was found to increase significantly after the deposition of 2.5 bilayers. So we have limited and stopped further polyelectrolyte deposition beyond this point.

Protein Adsorption on Untreated and Modified SF Fabrics

The interaction of proteins at the surface is a key factor in determining the hemocompatibility of any blood contacting biomaterial, and reducing the amount of nonspecific protein adsorption may be a most effective way to improve the performance of small diameter arterial prostheses. Reduction of protein adsorption can reduce the activation of the inflammatory and immune systems. So improved hemocompatibility of an ideal blood contacting biomaterial should allow less protein adsorption on its surface. In this study, the fibroin surfaces were exposed to FBS to investigate the effect of surface modification on protein adsorption. The amount of adsorbed FBS on the modified fibroin samples was reduced by 37% (SFF-1) and 55% (SFF-2), respectively, compared to the untreated SFF sample (Figure 10). These results are in agreement with the findings of Wendel and Ziemer[59] who suggested that heparin-modified surfaces lead to a reduced adsorption of selective plasma proteins as well as the maintenance of these proteins in their native state.

Hemolytic Effect of Untreated and Modified SF Fabrics

Hemolysis is a problem associated with the disruption of the membrane of red blood cells. This rupture leads to the loss of the internal cytoplasm, including hemoglobin, and the loss of cell function. For example, this can happen at the time of withdrawal, handling or storage of blood, or due to a range of different types of infections and chronic pathologies such as sickle cell anemia. Hemolysis can also occur due to the high osmotic pressures produced when red blood cells come into direct contact with water, or when foreign materials are used as artificial small diameter vascular prostheses and the blood cells experience high shear and turbulent forces.[60,61] The results of

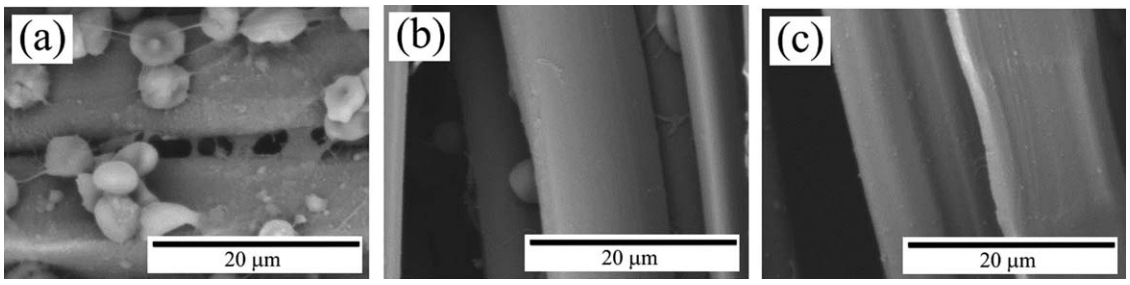

Figure 12. SEM photomicrographs of untreated and surface modified fibroin fabrics after exposure to whole blood. Magnification: ×5000. (a): Untreated SFF sample showing cell attachment, (b): SFF-1, and (c): SFF-2 surface treated samples show limited or no cell adhesion.

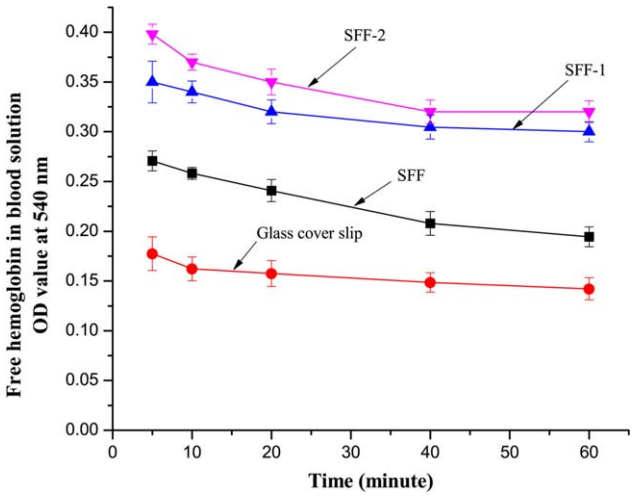

Figure 13. Rate of coagulation assay of untreated and surface modified SF fabrics at different time intervals. Data are shown as mean ($n = 3$), and the ± error bars = 1 standard deviation. [Color figure can be viewed in the online issue, which is available at wileyonlinelibrary.com.]

exposing the fibroin fabric samples to the HRBC suspension showed no significant hemolytic activity, except for the positive control (water). The hemolytic effect of each material was quantified by recording the absorbance of the supernatant liquid at 540 nm using UV–visible spectroscopy. It is clear from Figure 11 that there were significant differences ($P < 0.001$) in the average optical density of the hemoglobin between the positive control sample (where HRBC's were exposed to distilled water), and the three experimental samples and the isotonic PBS negative control.

The hemolytic index or hemolysis percent (HP) is a direct measure of free hemoglobin present in blood plasma after exposure to a given material or stress condition. The ASTM standard F756-00 classifies biomaterials as non-hemolytic (0–2% hemolysis), slightly hemolytic (2–5% hemolysis), and hemolytic (>5% hemolysis). Our results shown in Table III confirm that heparin modified fibroin fabrics are, according to this standard, classified as non-hemolytic, while the untreated sample is hemolytic.

As reported widely in the literature, SF is readily biocompatible when used in the form of thin films and electrospun mats. However, there are very few studies confirming the biocompatibility, and in particular, the hemocompatibility of SF in fibrous form. The most likely reason for this difference is that "as spun" silk fibers contain cytotoxic sericin gum that holds the pair of brins or filaments together. The sericin component needs to be completely removed to ensure 0% hemolysis. This can easily be achieved when precipitating thin films or electrospinning webs from a fibroin solution. The effectiveness of sericin removal by degumming a woven fabric is more challenging, as traces of sericin can remain trapped in the interlacements between the warp and weft yarns and filaments.

Rate of Coagulation of Modified Fibroin Fabrics

The coagulation of blood is initiated by thrombin that transforms fibrinogen into fibrin monomer, which under normal conditions forms long chain fibrin fibers, resulting in a stabilized clot or thrombus network containing red blood cells, white blood cells, and activated platelets.[62] Therefore, to evaluate the applicability of a biomaterial to be used in contact with blood, it is important to investigate the rate of this coagulation cascade on the biomaterial. SEM images of untreated and modified fibroin fabric samples after exposure to whole blood are presented in Figure 12. They clearly show that the surface of the unmodified fibroin fabric was covered with accumulated blood cells, while that of the surface modified and heparin immobilized samples (SFF-1 and SFF-2) showed almost no evidence of cellular adhesion. This limited *in vitro* experimental assay suggests that the heparin immobilized fibroin fabrics appear to be associated with a slower clotting process.

Figure 13 shows the mean optical density (OD) of free hemoglobin in the supernatant diluted blood following coagulation for different periods of time and exposure to distilled water. A higher OD value represents a higher hemoglobin concentration and suggests that the rate of clotting associated with the material is slower.

The OD values of the modified fibroin fabrics are higher at each time point compared to those of the untreated fibroin fabric and the glass cover slips. This may be due to the fact that the heparin is well incorporated within the modified fibroin fibers, but not with the unmodified fibroin. In contrast, under similar experimental conditions, glass cover slips displayed significantly faster clotting behavior after incubation for 60 min. The absorbance of hemoglobin in the case of a glass cover slip was 0.14, which is the lowest value because glass is one of the most thrombogenic materials.[63] These results revealed that all the modified fibroin fabrics possessed slower rates of coagulation than the unmodified fibroin samples. The enhanced anticoagulant property by heparin immobilization could be explained from two aspects: hydrophilicity and the negative charge density on the SF surfaces. According to the contact angle test results, the heparin immobilization increased the hydrophilicity and negative charge density of the fibroin fabric surfaces, which may have played a role in inhibiting the activities of some clotting factors of blood plasma.

CONCLUSIONS

In this study, heparin was immobilized onto modified fibroin fabric to enhance its hemocompatibility. The surface modification was achieved by the self-assembly deposition of 1.5 and 2.5 polyelectrolyte bilayers. SEM and AFM showed that the deposition of 2.5 bilayers followed by heparin immobilization generated a rougher surface topography compared to the 1.5 bilayers technique. Alcian Blue staining and toluidine blue assay confirmed the successful immobilization of heparin on the fibroin surfaces. The incorporation of heparin resulted in less protein adsorption, an acceptable hemolysis percent (<5%) and a slower rate of coagulation, as indicated by a higher concentration of free hemoglobin from the kinetic clotting time assay. These data indicate that the modified and heparin immobilized fibroin fabrics displayed superior hemocompatibility compared to untreated fibroin. In addition, this study has pointed out that the deposition of 2.5 bilayers of PAH and PAA is more

effective than 1.5 bilayers for enhancing the hemocompatibility of SF. This is the first time that the use of a polyelectrolyte layer-by-layer surface modification technique combined with heparin immobilization has been applied to SF fabrics. Future work will include other hemocompatibility and thrombogenicity tests such as the platelet adhesion test, aPTT test, and cytocompatibility assays.

ACKNOWLEDGMENTS

This work has been supported by the National Natural Science Foundation of China (Grant Nos. 51003014 and 31100682), the Fundamental Research Funds for the Central Universities, and the 111 Project "Biomedical Textile Materials Science and Technology" (Grant No. B07024).

REFERENCES

1. Li, G.; Zhang, F.; Liao, Y.; Yang, P.; Huang, N. *Colloids Surf. B. Biointerfaces* **2010**, *81*, 255.
2. Baguneid, M. S.; Seifalian, A. M.; Salacinski, H. J.; Murray, D.; Hamilton, G.; Walker, M. G. *Br. J. Surg.* **2006**, *93*, 282.
3. Kannan, R. Y.; Salacinski, H. J.; Edirisinghe, M. J.; Hamilton, G.; Seifalian, A. M. *Biomaterials* **2006**, *27*, 4618.
4. Lovett, M.; Cannizzaro, C.; Daheron, L.; Messmer, B.; Vunjak-Novakovic, G.; Kaplan, D. L. *Biomaterials* **2007**, *28*, 5271.
5. Zhu, Z.; Ohgo, K.; Watanabe, R.; Takezawa, T.; Asakura, T. *J. Appl. Polym. Sci.* **2008**, *109*, 2956.
6. Furuzono, T.; Ishihara, K.; Nakabayashi, N.; Tamada, Y. *J. Appl. Polym. Sci.* **1999**, *73*, 2541.
7. Furuzono, T.; Ishihara, K.; Nakabayashi, N.; Tamada, Y. *Biomaterials* **2000**, *21*, 327.
8. Chutipakdeevong, J.; Ruktanonchai, U. R.; Supaphol, P. *J. Appl. Polym. Sci.* **2013**, *130*, 3634.
9. Wang, X.; Wenk, E.; Matsumoto, A.; Meinel, L.; Li, C.; Kaplan, D. L. *J. Control. Release* **2007**, *117*, 360.
10. Wang, X.; Hu, X.; Daley, A.; Rabotyagova, O.; Cebe, P.; Kaplan, D. L. *J. Control. Release* **2007**, *121*, 190.
11. Wang, X.; Zhang, X.; Castellot, J.; Herman, I.; Iafrati, M.; Kaplan, D. L. *Biomaterials* **2008**, *29*, 894.
12. Wang, X.; Wenk, E.; Hu, X.; Castro, G. R.; Meinel, L.; Wang, X.; Li, C.; Merkle, H.; Kaplan, D. L. *Biomaterials* **2007**, *28*, 4161.
13. Hofmann, S.; Wong Po Foo, C. T.; Rossetti, F.; Textor, M.; Vunjak-Novakovic, G.; Kaplan, D. L.; Merkle, H. P.; Meinel, L. *J. Control. Release* **2006**, *111*, 219.
14. Nogueira, G. M.; Weska, R. F.; Vieira, W. C.; Polakiewicz, B.; Rodas, A. C. D.; Higa, O. Z.; Beppu, M. M. *J. Appl. Polym. Sci.* **2009**, *114*, 617.
15. Ki, C. S.; Kim, J. W.; Hyun, J. H.; Lee, K. H.; Hattori, M.; Rah, D. K.; Park, Y. H. *J. Appl. Polym. Sci.* **2007**, *106*, 3922.
16. Kim, H. J.; Kim, U. J.; Leisk, G. G.; Bayan, C.; Georgakoudi, I.; Kaplan, D. L. *Macromol. Biosci.* **2007**, *7*, 643.
17. Hofmann, S.; Hagenmüller, H.; Koch, A. M.; Müller, R.; Vunjak-Novakovic, G.; Kaplan, D. L.; Merkle, H. P.; Meinel, L. *Biomaterials* **2007**, *28*, 1152.
18. Meinel, L.; Betz, O.; Fajardo, R.; Hofmann, S.; Nazarian, A.; Cory, E.; Hilbe, M.; McCool, J.; Langer, R.; Vunjak-Novakovic, G.; Merkle, H. P.; Rechenberg, B.; Kaplan, D. L.; Kirker-Head, C. *Bone* **2006**, *39*, 922.
19. Meinel, L.; Karageorgiou, V.; Hofmann, S.; Fajardo, R.; Snyder, B.; Li, C.; Zichner, L.; Langer, R.; Vunjak-Novakovic, G.; Kaplan, D. L. *J. Biomed. Mater. Res., Part A* **2004**, *71*, 25.
20. Wang, Y.; Blasioli, D. J.; Kim, H. J.; Kim, H. S.; Kaplan, D. L. *Biomaterials* **2006**, *27*, 4434.
21. Hofmann, S.; Knecht, S.; Langer, R.; Kaplan, D. L.; Vunjak-Novakovic, G.; Merkle, H. P.; Meinel, L. *Tissue Eng.* **2006**, *12*, 2729.
22. Wang, Y.; Kim, U. J.; Blasioli, D. J.; Kim, H. J.; Kaplan, D. L. *Biomaterials* **2005**, *26*, 7082.
23. Nakazawa, Y.; Sato, M.; Takahashi, R.; Aytemiz, D.; Takabayashi, C.; Tamura, T.; Enomoto, S.; Sata, M.; Asakura, T. *J. Biomater. Sci. Polym. Ed.* **2011**, *22*, 195.
24. Yang, X.; Wang, L.; Guan, G.; King, M. W.; Li, Y.; Peng, L.; Guan, Y.; Hu, X. *J. Biomater. Appl.* **2014**, *28*, 676.
25. Enomoto, S.; Sumi, M.; Kajimoto, K.; Nakazawa, Y.; Takahashi, R.; Takabayashi, C.; Asakura, T.; Sata, M. *J. Vasc. Surg.* **2010**, *51*, 155.
26. Tamada, Y. *J. Appl. Polym. Sci.* **2003**, *87*, 2377.
27. Wang, S.; Lian, X. J.; Chen, X. M.; Li, E. L.; Zhu, H. S. *Eur. Cell. Mater.* **2007**, *14*, 94.
28. Yagi, T.; Sato, M.; Nakazawa, Y.; Tanaka, K.; Sata, M.; Itoh, K.; Takagi, Y.; Asakura, T. *J. Artif. Organs* **2011**, *14*, 89.
29. Du, Y. J.; Brash, J. L.; McClung, G.; Berry, L. R.; Klement, P.; Chan, A. K. C. *J. Biomed. Mater. Res., Part A* **2007**, *80*, 216.
30. Ki Dong, P.; Won Gon, K.; Jacobs, H.; Okano, T.; Sung Wan, K. *J. Biomed. Mater. Res.* **1992**, *26*, 739.
31. Serra, A.; Esteve, J.; Reverter, J. C.; Lozano, M.; Escolar, G.; Ordinas, A. *Thromb. Res.* **1997**, *87*, 405.
32. Young, E.; Venner, T.; Ribau, J.; Shaughnessy, S.; Hirsh, J.; Podor, T. J. *Thromb. Res.* **1999**, *96*, 373.
33. Hirsh, J. *Am. Heart J.* **1998**, *135*, S336.
34. Decher, G. *Science* **1997**, *277*, 1232.
35. Lojou, E.; Bianco, P. *Langmuir* **2004**, *20*, 748.
36. Kotov, N. A. *Nanostruct. Mater.* **1999**, *12*, 789.
37. Shiratori, S. S.; Rubner, M. F. *Macromolecules* **2000**, *33*, 4213.
38. Schmitt, J.; Gruenewald, T.; Decher, G.; Pershan, P. S.; Kjaer, K.; Loesche, M. *Macromolecules* **1993**, *26*, 7058.
39. Picart, C.; Elkaim, R.; Richert, L.; Audoin, F.; Arntz, Y.; Cardoso, M. D. S.; Schaaf, P.; Voegel, J. C.; Frisch, B. *Adv. Funct. Mater.* **2005**, *15*, 83.
40. Mallwitz, F.; Laschewsky, A. *Adv. Mater.* **2005**, *17*, 1296.
41. Podsiadlo, P.; Qin, M.; Cuddihy, M.; Zhu, J.; Critchley, K.; Kheng, E.; Kaushik, A. K.; Qi, Y.; Kim, H.-S.; Noh, S.-T.; Arruda, E. M.; Waas, A. M.; Kotov, N. A. *Langmuir* **2009**, *25*, 14093.
42. Johansson, E.; Blomberg, E.; Lingstroüm, R.; Wågberg, L. *Langmuir* **2009**, *25*, 2887.
43. Xiao, W.; Yiwei, Q.; Andrew, J. C.; James, T. T.; Afsie, S.; Zhidao, X. *Biomed. Mater.* **2011**, *6*, 035010.

44. Park, K. D.; Piao, A. Z.; Jacobs, H.; Okano, T.; Kim, S. W. *J. Polym. Sci., Part A: Polym. Chem.* **1991**, *29*, 1725.
45. Li, J.; Lin, F.; Li, L.; Li, J.; Liu, S. *Macromol. Chem. Phys.* **2012**, *213*, 2120.
46. Zhao, Y.; Wang, S.; Guo, Q.; Shen, M.; Shi, X. *J. Appl. Polym. Sci.* **2013**, *127*, 4825.
47. Ren, Z.; Chen, G.; Wei, Z.; Sang, L.; Qi, M. *J. Appl. Polym. Sci.* **2013**, *127*, 308.
48. He, Q.; Zhang, J.; Shi, J.; Zhu, Z.; Zhang, L.; Bu, W.; Guo, L.; Chen, Y. *Biomaterials* **2010**, *31*, 1085.
49. Lin, Y.-S.; Haynes, C. L. *Chem. Mater.* **2009**, *21*, 3979.
50. Lee, K. Y.; Ha, W. S.; Park, W. H. *Biomaterials* **1995**, *16*, 1211.
51. Meng, Z. X.; Zheng, W.; Li, L.; Zheng, Y. F. *Mater. Sci. Eng. C* **2010**, *30*, 1014.
52. Szebeni, J. *Eur. J. Nanomed.* **2012**, *33*.
53. Rajkhowa, R.; Wang, L.; Kanwar, J. R.; Wang, X. *J. Appl. Polym. Sci.* **2011**, *119*, 1339.
54. Liu, S.; Dong, C.; Lu, G.; Lu, Q.; Li, Z.; Kaplan, D. L.; Zhu, H. *Acta Biomater.* **2013**, *9*, 8991.
55. Liu, X.-Y.; Zhang, C.-C.; Xu, W.-L.; Ouyang, C.-X. *Mater. Lett.* **2009**, *63*, 263.
56. Dowling, D. P.; Miller, I. S.; Ardhaoui, M.; Gallagher, W. M. *J. Biomater. Appl.* **2011**, *26*, 327.
57. Lee, J. H.; Lee, H. B. *J. Biomed. Mater. Res.* **1998**, *41*, 304.
58. Sethuraman, A.; Han, M.; Kane, R. S.; Belfort, G. *Langmuir* **2004**, *20*, 7779.
59. Wendel, H. P.; Ziemer, G. *Eur. J. Cardiothorac. Surg.* **1999**, *16*, 342.
60. Dey, R. K.; Ray, A. R. *Biomaterials* **2003**, *24*, 2985.
61. Shim, D.; Wechsler, D. S.; Lloyd, T. R.; Beekman Iii, R. H. *Cathet. Cardiovasc. Diagn.* **1996**, *39*, 287.
62. Smith, B. S.; Yoriya, S.; Grissom, L.; Grimes, C. A.; Popat, K. C. *J. Biomed. Mater. Res., Part A* **2010**, *95A*, 350.
63. Gajjar, C. MS Thesis, North Carolina State University, Raleigh, USA, **2011**.